Clinical Case Report

Medicine®

OPEN

Two novel *TSC2* mutations in pediatric patients with tuberous sclerosis complex

Case report

Shan Gao, MD[a,b], Zhiling Wang, MD[a,b,*], Yongmei Xie, MD[a,b]

Abstract

Rationale: Tuberous sclerosis complex (TSC) is a rare autosomal dominant disorder. The *TSC1* and *TSC2* genes have been identified as pathogenic genes.

Patient concerns: In this report, we are discussing a novel frameshift mutation and a novel missense mutation in the *TSC2* gene.

Diagnoses: The two cases discussed in this study met the latest diagnostic criteria for TSC published by the International Tuberculosis Sclerosis Complex Consensus Conference in 2012.

Interventions: High-throughput sequencing and multiplex ligation-dependent probe amplification (MLPA) were used to examine tuberous sclerosis complex (TSC)-related genes (*TSC1* and *TSC2*) and their splicing regions using peripheral blood DNA from two probands in two families with TSC and to identify the genetic mutation sites. Amplification primers were designed for the mutation sites, and polymerase chain reaction and Sanger sequencing were used to verify the peripheral blood DNA sequences from the probands and their parents.

Outcome: Proband 1 had the c.1228 (exon 12)_c.1229 (exon 12) insG (p.L410RfsX11) heterozygous mutation in the *TSC2* gene (chr16), which was a new frameshift mutation. Proband 2 had the c.4925G>A (exon 38) (p.G1642D) heterozygous mutation in the *TSC2* gene (chr16), which was a new missense mutation.

Lessons: These two novel mutations may be pathogenic mutations for TSC, and their association with the disease needs to be further verified by mutant protein function cell model and animal model.

Abbreviations: ACTH = adrenocorticotropic hormone, EDTA = ethylenediaminetetraacetic acid, EEG = electroencephalogram, GAP = GTPase activator protein, Indel = insertion–deletion, LM-PCR = ligation-mediated polymerase chain reaction, MLPA = multiplex ligation-dependent probe amplification, mTOR = mammalian target of rapamycin, S6K = S6 kinase, SEGAs = subepithelial giant cell astrocytomas, SENS = subepithelial nodules, SIFT = scale invariant feature transform, SNP = single nucleotide polymorphism, T4PNK = T4 polynucleotide kinase, TSC = tuberous sclerosis complex.

Keywords: child, frameshift mutation, missense mutation, *TSC2* gene, tuberous sclerosis complex

1. Introduction

Tuberous sclerosis complex (TSC; OMIM 613254) is a rare autosomal dominant disorder that is characterized by the formation of a hamartoma in multiple tissues and organs, which often include the brain, skin, heart, kidneys, lungs, and eyes.[1] TSC can have diverse clinical manifestations, which are age-related. For example, epilepsy, mental retardation or retrogression, autism, angiofibromatosis, shagreen patch, periungual fibromas, cardiac rhabdomyoma, renal angiomyolipoma, and lymphangioleiomyoma occur more frequently in adults than in children, whereas heart hamartomas are more common in children.[2] The annual incidence in neonates is approximately 1:6000 to 1:10,000[3]; sporadic cases account for approximately 2/3 of this total,[4] which suggests a high rate of spontaneous mutations. Currently, the *TSC1* and *TSC2* genes, which are located on chromosomes 9q34.3 and 16p13.3, respectively, have been identified as pathogenic genes. *TSC1* encodes a 130-kDa protein TSC1/hamartin and *TSC2* encodes a 200-kDa protein TSC2/tuberin.[2] The pathogenic mutations of the *TSC1* and *TSC2* genes include frameshift mutations, missense mutations, nonsense mutations, splicing mutations, deletions, and insertions. Neither gene has mutation hot spots. This article discusses a novel frameshift mutation and a novel missense mutation in the *TSC2* gene.

2. Materials and methods

2.1. Subjects

The proband in Family 1 was male, 8 months and 3 days old, and ethnically Han from Leshan City, Sichuan Province. No abnormalities were reported during his mother's pregnancy. The child was the second live-born progeny of 4 pregnancies (G4P2), was delivered at full term by cesarean section, and had no history of asphyxia. Abdominal and back discoloration was found 2 to 3 months after birth, and repeated involuntary

Editor: N/A.

The authors have no conflicts of interest to disclose.

[a] Department of Pediatric Neurology and Gastroenterology, West China Second University Hospital, [b] Key Laboratory of Obstetric & Gynecologic and Pediatric Diseases and Birth Defects of Ministry of Education, Sichuan University, Chengdu, P.R. China.

[*] Correspondence: Zhiling Wang, Department of Pediatrics, Sichuan University West China Second University Hospital, No. 20, Section 3, Ren Min Nan Lu Road, Chengdu, Sichuan 610041, P.R. China (e-mail: wang_zhi_ling@126.com).

Medicine (2018) 97:29(e11533)

Received: 10 April 2018 / Accepted: 20 June 2018

http://dx.doi.org/10.1097/MD.0000000000011533

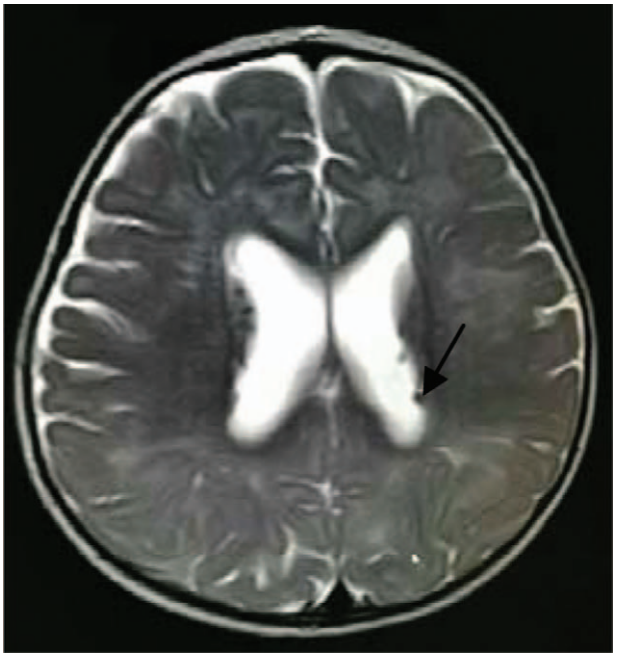

Figure 1. Brain MRI features of the proband in Family 1: Bilateral multiple subependymal nodules of the lateral ventricles.

nodding- and embracing-like motions were observed 7 months after birth and occurred continuously for 1 to 3 minutes per episode at a rate of more than 10 episodes/day. At 8 months after birth, a video electroencephalogram (EEG) showed frequent multifocal (slow) and (multiple) spike (slow) waves, indicating that the clinical symptoms could have been due to seizures. Brain MRI showed multiple patchy abnormal signals in the bilateral hemispheres and bilateral multiple subependymal nodular shadows of the lateral ventricles, indicating the possibility of TSC (Fig. 1). Echocardiography showed septal and left intraventricular strong echoes (suggesting rhabdomyomas), and chest and abdominal noncontrast CT scans showed left renal cysts. The TSC gene detection analysis showed the c.1228 (exon 12)_c.1229 (exon 12) insG (p.L410RfsX11) heterozygous mutation in the *TSC2* gene (chr16). The development of the patient was delayed; the patient could lift his head and occasionally laugh upon stimulation when he was 4 months old and could sit with support, but he could not sit independently when he was 8 months old, which was the time of the examination. After the onset of the disease, the patient showed developmental retrogression, such as instability of the neck when held upright and an inability to laugh upon stimulation. The parents of the proband and the elder brother (3 years old) have no TSC-related symptoms.

The proband in Family 2 was male, 5 months and 3 days old, and ethnically Han from Jiangkou Township, Pingchang, Sichuan Province. No abnormalities were reported during the mother's pregnancy. The child was the second live-born progeny of 2 pregnancies (G2P2), was delivered at full term by cesarean section, and had no history of asphyxia. In the second month after birth, discoloration of the forehead, neck, abdomen, and lower extremities was found and gradually increased. Repeated involuntary nodding- and embracing-like motions were observed 4 months after birth, and they occurred continuously for 1 to 2 minutes per episode at a rate of 3 to 4 episodes/day. At 5 months after birth, video EEG showed frequent multifocal sharp (slow), (multiple) spike (slow) waves, and slow waves, indicating that the clinical symptoms could have been due to seizures. The brain MRI showed various sizes of bilateral subependymal nodular shadows of the lateral ventricles and patchy abnormal signals in the deep bilateral temporal lobes, inferior horn of the lateral ventricle, frontal lobe, and parietal lobe, thus indicating the possibility of TSC (Fig. 2). Echocardiography showed right intraventricular occupancy (rhabdomyomas?), and chest noncontrast CT scanning showed pulmonary inflammation, right pleural constriction, and slight thickening. Ultrasound examination of the liver, gallbladder, pancreas, spleen, and urinary system revealed no abnormalities. TSC gene detection analysis showed the c.4925G>A (exon 38) (p.G1642D) heterozygous mutation in the *TSC2* gene (chr16). The patient could lift his head when he was 3 months old, but he could not roll over at the time of the examination. After the onset of the disease, the patient showed developmental retrogression, such as instability of the neck when held upright and an inability to laugh upon stimulation. The parents of the proband and the elder sister have no TSC-related symptoms.

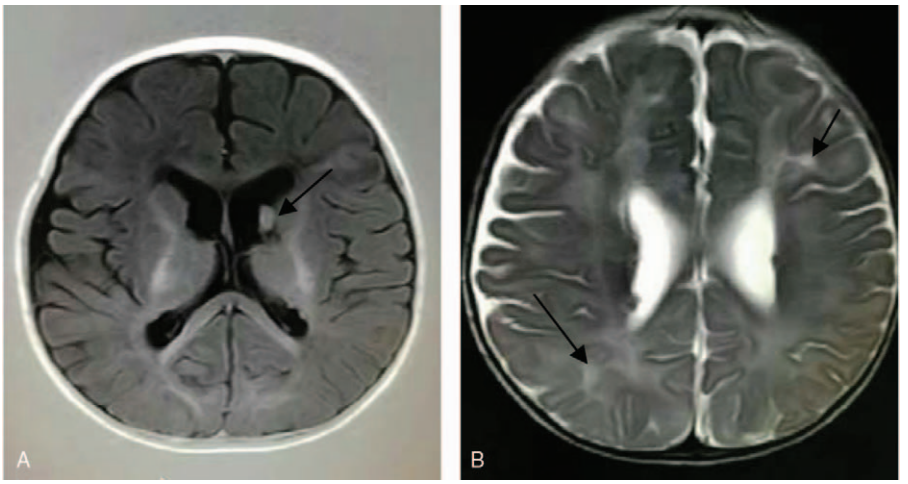

Figure 2. Brain MRI features of the proband in Family 2: (A) A subependymal giant cell astrocytoma of the right ventricle; (B) an abnormal patchy signal near the inferior horn of the lateral ventricle, frontal lobe, and parietal lobe.

This study complied with the ethical standards issued by the Institutional Review Board and was approved by the Ethics Committee, West China Second Hospital, Sichuan University. The patients' guardians signed informed consent forms and agreed to publish the examination results for medical research purposes.

2.2. Experimental methods

2.2.1. Peripheral blood genomic DNA extraction. After obtaining informed consent, 2 mL of peripheral blood was taken from the probands and the parents of the probands, with ethylenediaminetetraacetic acid (EDTA) added for anticoagulation treatment. Genomic DNA was extracted using the BloodGen Midi Kit (CWBIO, Beijing, China) according to the manual.

2.2.2. Next-generation sequencing. Based on the OMIM database and the literature, we designed Roche NimbleGen capture probes using the exon regions of the TSC-associated *TSC1* and *TSC2* genomic sequences for target gene whole exome capture.

Library preparation

a. Fragmentation of the genome: Genomic DNA was sheared to approximately 200 bp using a Cavoris instrument.
b. End repair: End repair of fragmented DNA was achieved using Klenow fragments, the T4 DNA polymerase, and the T4 polynucleotide kinase (T4PNK).
c. 3′-Adenosylation: The polymerase system added the A base at the 3′ end of the repair product obtained in step b.
d. Ligation of adapters: The T4 DNA ligase reaction system was used to ligate the adapter to the "A" product obtained in step c by incubation for the specified amount of time in a Thermo mixer at an appropriate temperature.
e. Amplification: The ligation product was amplified by 4 to 6 rounds of ligation-mediated polymerase chain reaction (LM-PCR).
f. Hybridization: The library was mixed with the probes in a hybridization system at 65°C for 60 to 68 hours of hybridization.
g. Washing of magnetic beads and DNA elution: After incubating the hybridization samples with streptomycin beads, the eluent was used to elute the DNA.
h. Amplification of the eluted product: The eluted product was amplified by 10 rounds of LM-PCR.

Illumina platform sequencing

a. Sequencing was performed via the standardized sequencing workflow of the Illumina HiSeq 2500 platform.
b. The raw data were obtained by analyzing the original sequencing data using the official BclToFastq software from Illumina.
c. Data analysis
   - Yield analysis of raw data: Adapter contamination and low-quality data were removed.
   - Alignment: The data obtained in step i were aligned to the reference sequence (the Burrows–Wheeler Alignment tool, BWA, was used for the alignment) using the hg19 genome as the reference genome.
   - Single nucleotide polymorphism (SNP) detection and annotation: The results were analyzed using the SAMtools software.
   - Insertion–deletion (Indel) detection and annotation: The Pindel software was used to analyze the results.
   - False-positive filtering: According to the quality of the mutation analysis and the sequencing depth, the detected SNPs and Indels were filtered and screened to obtain high-quality and reliable mutations.
   - Mutation annotation: Based on the locations of the SNPs and Indels in the gene, the effects on amino acids, splicing, untranslated regions, and intron mutations were determined.
   - Prediction of the influence of the selected mutations on protein function: We used algorithms based on the homologous alignment and conservation of the protein structure and applied the scale invariant feature transform (SIFT) algorithm to predict the influence of the selected mutation on the protein.
   - Splicing alternation predictions for mutations near the splice site.

2.2.3. Sanger sequencing verification. Primers were designed based on the sequences of the TSC sites for verification, and PCR amplification was performed. The PCR reaction conditions were as follows: predenaturation at 95°C for 5 minutes; 30 cycles of denaturation at 95°C for 30 seconds, annealing at 60°C for 30 seconds, and extension at 72°C for 30 seconds; and an additional extension step at 72°C for 10 minutes to ensure that the PCR reaction was complete and to increase the amplification yield. The PCR system volume was 50 μL, and the primer sequences are presented in Table 1. For the gene sequence analysis, PCR amplification products of the TSC sites for verification were sequenced using the ABI 3730XL sequencer with the original PCR primers as the sequencing primers. The gene sequence analysis was performed using the DNASTAR software for sequence analysis and alignment.

3. Results

The targeted TSC genes in the probands were sequenced, and multiplex ligation-dependent probe amplification (MLPA) was used to detect deletions or duplications. Candidate sites were screened by database searching and bioinformatics analysis. For known point mutations, cosegregation analysis within the family was conducted via Sanger sequencing. For novel mutation sites, cosegregation analysis was conducted within the family, and the sites were verified in normal individuals to eliminate the possibility of polymorphisms. Our results showed that the

Table 1

Primer sequences to verify the sites in the *TSC* genes.

Family	Primer name	Base sequence	Annealing temperature, °C	Amplification product size, bp	mRNA alignment template
1	GN541-8F-1	TCTCCATGCGGTGGGTGTGTAGC	60	1360	TSC:NM_000548c.1228_c.1229insGp.L410Rfs*11
	GN541-8R-2	CTCTGCGGGAGCACGTGCACAAC			
2	F	CTCCGCCCAGTCTCAGTGAGTCCC	60	1278	NM_000548
	R	ACCCAGTCTGCACTTGCCAGTTACTCC			

Figure 3. Results of next-generation sequencing of the proband in family 1 (the long box marks the mutation site).

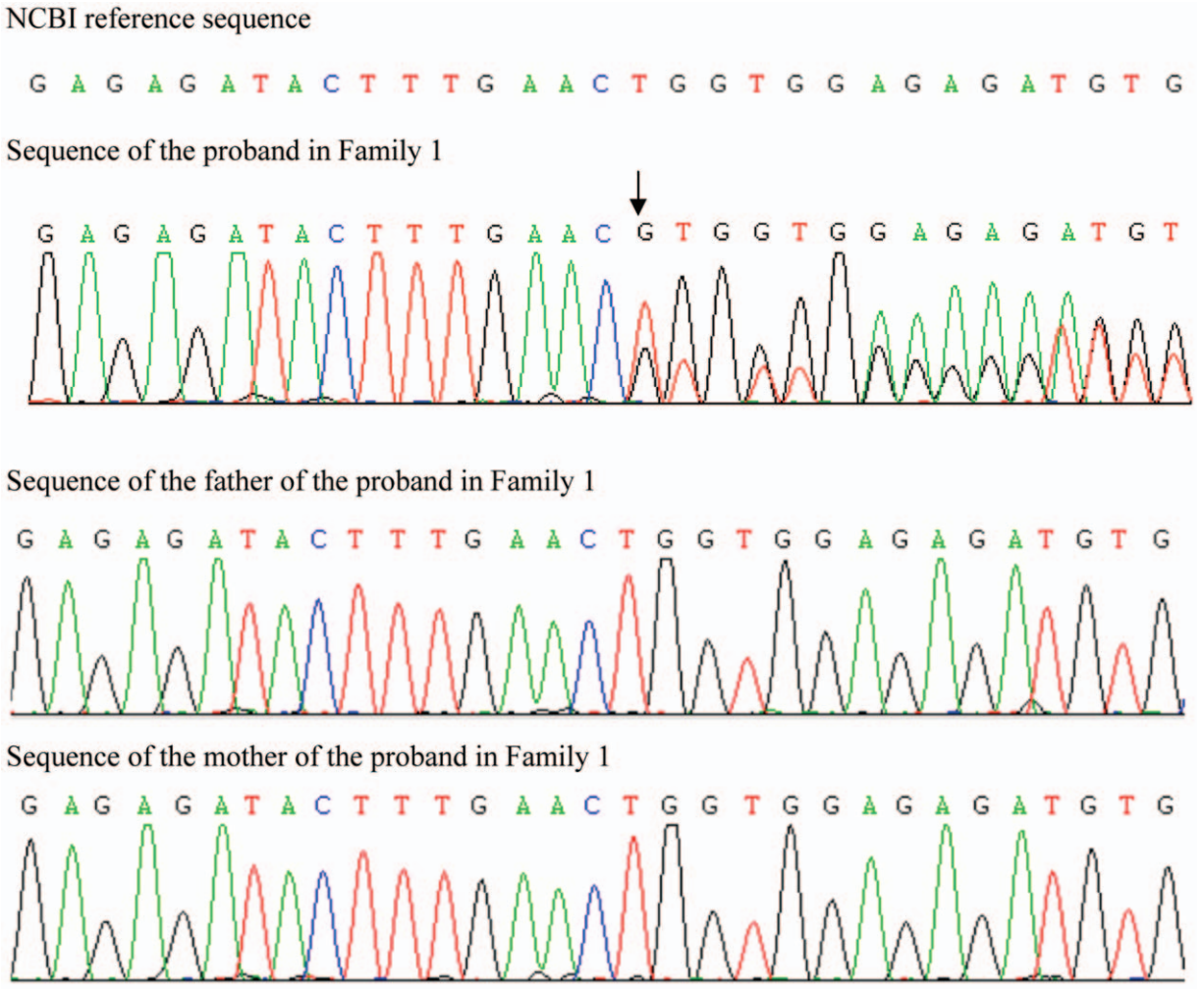

Figure 4. Sequencing results of the c.1228–1229 insG heterozygous mutation in the TSC2 gene c.1228 (exon 12)_c.1229 (exon 12) insG in the proband of Family 1 (the arrow indicates the mutation site).

Figure 5. Results of next-generation sequencing of the proband in Family 2 (the long box marks the mutation site).

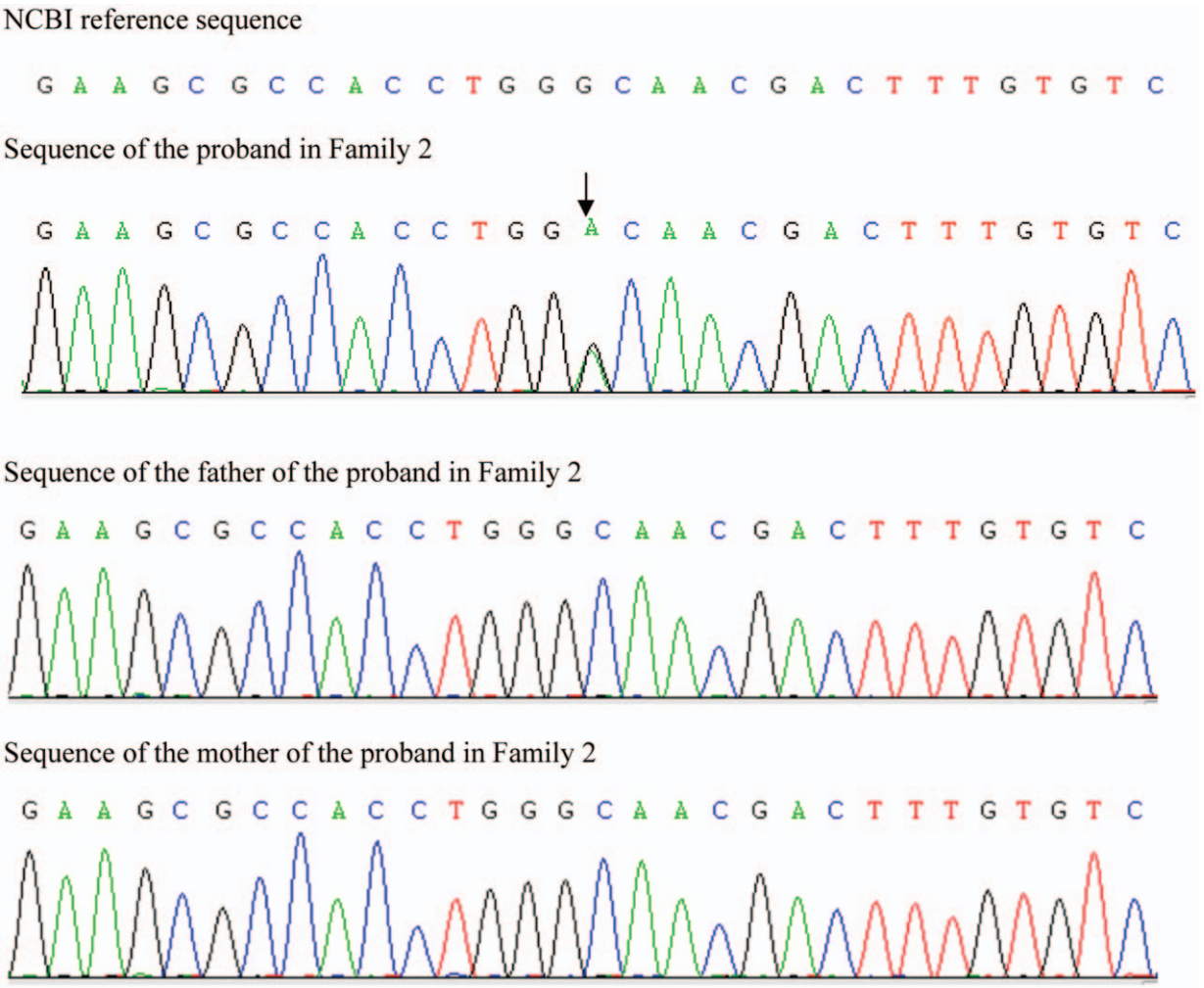

Figure 6. Sequencing results of the c.4925 G>A heterozygous mutation in the TSC2 gene c.4925G>A (exon 38) in the proband of Family 2 (the arrow indicates the mutation site).

proband in Family 1 had the c.1228 (exon 12)_c.1229 (exon 12) insG (p.L410RfsX11) heterozygous mutation in the *TSC2* gene (chr16) (Figs. 3 and 4), which changed the leucine (L) at position 410 to arginine (R) and led to an early termination at position 420, resulting in a frameshift mutation. Proband 2 had the c.4925G>A (exon 38) (p.G1642D) heterozygous mutation in the *TSC2* gene (chr16) (Figs. 5 and 6), which changed the amino acid at position 1642 from glycine (G) to aspartic acid (D), resulting in a missense mutation. Protein structure predictions using Provean, Polyphen2, Sift, Mutationtaster, M-CAP, and REVEL suggest that this latter mutation may be harmful to the protein structure. The pathogenicity of the 2 mutations has not been reported in the literature. No abnormalities were found in the corresponding sites in the parents of the 2 probands.

These 2 mutations were not previously reported to be associated with TSC in the OMIM, HGMD, and Clinvar databases and were not included in the databases for normal human subjects (DYDF, dbSNP, The 1000 Genomes Project, Thousand Genomes In the South, Thousand Genomes In the North, and ExAC), which suggests that they were new mutations.

4. Discussion

The TSC pathogenic genes *TSC1* and *TSC2* belong to the tumor suppressor genes. To date, more than 1000 gene mutation sites have been reported, covering almost all exons of the *TSC1* and *TSC2* genes. *TSC2* mutations account for approximately 60% of TSC mutations, and *TSC1* mutations account for approximately 30%.[5,6] However, no mutations have been found in 10% to 25% of all clinically diagnosed TSC patients.[7] Possible causes include insufficient detection sensitivity, mutations in introns or promoter regions, low-abundance somatic cell chimeric mutants in *TSCs*, and the presence of unidentified gene loci, such as the *TSC3* gene.[8]

The *TSC1*-encoded Hamartin and TSC2-encoded tuberin proteins have high affinity and form a heterodimer in the cytoplasm. Mutations in the *TSC1* or *TSC2* genes affect the function of the TSC1–TSC2 complex (also known as the hamartin–tuberin complex), resulting in an abnormality in the GAP domain (GTPase activator protein) of *TSC2*. In turn, this abnormality leads to the abnormal activation of the mammalian target of rapamycin (mTOR) signal transduction pathway and the reduced dephosphorylation of the ribosomal protein S6 kinase (S6K), which weakens or eliminates the inhibition of cell proliferation, angiogenesis, and metabolism and results in rapid cell proliferation and hamartoma lesions.[9–12] At present, there are many reports both in China and abroad on *TSC2* gene frameshift mutations and missense mutations that lead to abnormalities in the GAP domain and subsequently disease onset.[13–15] The GAP domain is located at amino acids 1531 to 1758. The proband of Family 1 had the c.1228 (exon 12)_c.1229 (exon 12) insG (p.L410RfsX11) heterozygous mutation in the *TSC2* gene (chr16); the amino acid sequence was prematurely terminated at position 420 in front of the GAP domain, resulting in the absence of the entire GAP domain, which could be the pathogenic cause. The proband of Family 2 had the c.4925G>A (exon 38) (p.G1642D) heterozygous mutation in the *TSC2* gene (chr16), and they changed the glycine (G) located at position 1642 of the GAP domain to aspartic acid (D). Structural abnormality of the GAP domain is the pathogenic cause. These 2 mutations were not previously reported to be associated with TSC in the OMIM, HGMD (www.hgmd.cf.ac.uk/ac/index.php), and Clinvar databases and were not included in the databases for normal human subjects (DYDF, dbSNP, The 1000 Genomes Project, Thousand Genomes In the South, Thousand Genomes In the North, and ExAC), which suggests that they were new mutations. After analyzing the amino acid structure and the clinical manifestations of the proband, we speculated that these 2 mutations were new pathogenic mutations.

The 2 cases discussed in this study met the latest diagnostic criteria for TSC published by the International Tuberculosis Sclerosis Complex Consensus Conference in 2012[7] and had the following similarities. Similarity in age: the proband in Family 1 is 11 months old at present, and the proband in Family 2 is now 1 year old. Both had similar ages of onset; the former had an age of onset at 7 months after birth, and the latter had an age of onset at 4 months after birth, both of which were before the age of 1 year. There is damage to the central nervous system, including spasmodic seizures, and retrogression of mental and motor development. Both are associated with heart and skin lesions. Both had heterozygous *TSC2* gene mutations that affected the GAP domain. The elder brother who shared the same parents as the proband in Family 1 and the elder sister who shared the same parents as the proband in Family 2 had no clinical manifestations of TSC. Similarity in treatment response: Both patients received adrenocorticotropic hormone (ACTH) shock therapy and a regular administration of Levetiracetam but still had repeated seizures. Damage to the central nervous system is the most prominent manifestation of the 2 patients in this study and is the most prominent feature of pediatric TSC.

TSC nervous system damage manifests primarily as intractable epilepsy, autism, cognitive disorders, hydrocephalus, and other nervous system dysfunctions and abnormal mental behaviors.[16] Neurological damages caused by *TSC2* mutations are more common than those caused by *TSC1* mutations.[17] Typical pathological manifestations include cortical tubers, subepithelial nodules (SENS), and subepithelial giant cell astrocytomas (SEGAs).[18] Currently, cortical tubers and SEGAs are believed cause neurological symptoms, whereas SENS does not cause these symptoms. Cortical tubers are the main cause of epilepsy in TSC patients and may also be the cause of cognitive impairment in patients with TSC. Nodules can be single or multiple and often involve the frontal lobes and occipital lobes as well as the cerebellum.[19] Nodular changes in the fetal nervous system can be detected by imaging studies as early as the 20th week of pregnancy.[3] Currently, mutations in *TSC1* and *TSC2* are believed to occur at 7 to 20 weeks of gestation and to affect the normal development of neural progenitor cells, leading to abnormal cell types and tissue structures.

In addition to genetic mutations that affect the development of nerve cells, inflammatory cells play an important role in the pathogenesis of TSC. The detection of inflammatory markers in cerebral cortical tubers identified tumor necrosis factor-α, NF-kappa B, and cell adhesion factor ICAM-1[20] the above inflammatory factors were even found in fetal cortical nodule specimens, thus suggesting a pathogenic role of inflammatory factors in TSC. Analyzing the gene expression in cortical tubers demonstrated that inflammatory pathways were activated in TSC lesions,[21] proving that various inflammatory cells played an important role in the pathogenesis of TSC. Therefore, the specific involvement of inflammatory cells in the mTOR pathway needs to be further investigated. In conclusion, activation of the inflammatory cascade may be responsible for dynamic changes in TSC lesions and may contribute to progressive neuronal and glial cell damage in TSC patients.

More than 80% of patients with TSC are estimated to have epilepsy and can have various episodes. Moreover, epilepsy is

difficult to treat in many patients, and the mechanism underlying the epilepsy is not clear. In most TSC patients, a correlation is usually found between the location of the nodule and the affected area, with the nodule considered to be an epileptogenic lesion. Because multiple nodules can be present, TSC patients may develop multifocal or generalized seizure syndromes, such as infantile spasms or Lennox–Gastaut syndrome. Repeated seizures in patients with TSC may be caused by mutations in the *TSC1/TSC2* genes, abnormal cortical cell structures, changes in synaptic connections, changes in the expression of neurotransmitter receptors or ion channels, abnormal expression of growth factors, and excessive proinflammatory responses. Thus, the surgical removal of nodules should, logically, reduce seizures. However, recent studies that placed a detection electrode on the nodules and the surrounding cortex found no abnormal discharge in the nodular region, whereas the surrounding cortical tissue showed significant epileptic activity. This finding suggests that the epileptogenic lesion may not be in the nodule itself but may instead be in the cortex around the nodule[22] and may cause uncontrolled seizure symptoms in some patients after nodule resection.

In summary, children's TSC most often afflicts the nervous system, which not only leads to severe abnormalities in mental and motor development but also often causes death. This disease causes serious pain to the child, burdens to family and society. Therefore, prenatal examination is particularly important. The 2 new mutations detected in this study were presumed to be pathogenic mutations, which enriched the spectrum of gene mutations. However, genetic mutations eventually lead to the pathological process of injury, which is under the effects of various factors, including the internal and external environments. The pathogenesis is very complex and remains unclear; thus, the functions of the mutated proteins need to be validated using cell and animal models. The discovery of new mutations not only provides a basis for prenatal genetic diagnosis for the affected family but also more research entry points.

Author contributions

Conceptualization: Shan Gao, Yongmei Xie.
Data curation: Shan Gao, Yongmei Xie.
Formal analysis: Shan Gao.
Funding acquisition: Zhiling Wang.
Investigation: Shan Gao.
Methodology: Shan Gao.
Writing – original draft: Shan Gao.
Writing – review & editing: Zhiling Wang.

References

[1] Ismail NF, Nik Abdul Malik NM, Mohseni J, et al. Two novel gross deletions of TSC2 in Malaysian patients with tuberous sclerosis complex and TSC2/PKD1 contiguous deletion syndrome. Jpn J Clin Oncol 2014;44:506–11.
[2] Orlova KA, Crino PB. The tuberous sclerosis complex. Ann NY Acad Sci 2010;1184:87–105.
[3] Osborne JP, Fryer A, Webb D. Epidemiology of tuberous sclerosis. Ann NY Acad Sci 1991;615:125–7.
[4] Huang CH, Peng SS, Weng WC, et al. The relationship of neuroimaging findings and neuropsychiatric comorbidities in children with tuberous sclerosis complex. J Formos Med Assoc 2015;114:849–54.
[5] Jones AC, Daniells CE, Snell RG, et al. Molecular genetic and phenotypic analysis reveals differences between TSC1 and TSC2 associated familial and sporadic tuberous sclerosis. Hum Mol Genet 1997;6:2155–61.
[6] Jones AC, Shyamsundar MM, Thomas MW, et al. Comprehensive mutation analysis of TSC1 and TSC2 and phenotypic correlations in 150 families with tuberous sclerosis. Am J Hum Genet 1999;64: 1305–15.
[7] Krueger DA, Northrup H. International Tuberous Sclerosis Complex Consensus GroupTuberous sclerosis complex surveillance and management: recommendations of the 2012 International Tuberous Sclerosis Complex Consensus Conference. Pediatr Neurol 2013;49:255–65.
[8] Qin W, Kozlowski P, Taillon BE, et al. Ultra deep sequencing detects a low rate of mosaic mutations in tuberous sclerosis complex. Hum Genet 2010;127:573–82.
[9] Astrinidis A, Henske EP. Tuberous sclerosis complex: linking growth and energy signaling pathways with human disease. Oncogene 2005;24:7475–81.
[10] Huang J, Manning BD. The TSC1-TSC2 complex: a molecular switchboard controlling cell growth. Biochem J 2008;412:179–90.
[11] De Waele L, Lagae L, Mekahli D. Tuberous sclerosis complex: the past and the future. Pediatr Nephrol 2015;30:1771–80.
[12] Mazhab-Jafari MT, Marshall CB, Ho J, et al. Structure-guided mutation of the conserved G3-box glycine in Rheb generates a constitutively activated regulator of mammalian target of rapamycin (mTOR). J Biol Chem 2014;289:12195–201.
[13] Mayer K, Goedbloed M, Van Zijl K, et al. Characterisation of a novel TSC2 missense mutation in the GAP related domain associated with minimal clinical manifestations of tuberous sclerosis. J Med Genet 2004;41:e64.
[14] Yu Z, Zhang X, Guo H, et al. A novel TSC2 mutation in a Chinese family with tuberous sclerosis complex. J Genet 2014;93:169–72.
[15] Pan YC, Wu WQ, Xie JS, et al. Two novel TSC2 frameshift mutations in tuberous sclerosis complex. Zhongguo Dang Dai Er Ke Za Zhi 2017;19:308–12.
[16] Napolioni V, Moavero R, Curatolo P. Recent advances in neurobiology of tuberous sclerosis complex. Brain Dev 2009;31:104–13.
[17] Dabora SL, Jozwiak S, Franz DN, et al. Mutational analysis in a cohort of 224 tuberous sclerosis patients indicates increased severity of TSC2, compared with TSC1, disease in multiple organs. Am J Hum Genet 2001;68:64–80.
[18] Mizuguchi M, Takashima S. Neuropathology of tuberous sclerosis. Brain Dev 2001;23:508–15.
[19] Vaughn J, Hagiwara M, Katz J, et al. MRI characterization and longitudinal study of focal cerebellar lesions in a young tuberous sclerosis cohort. AJNR Am J Neuroradiol 2013;34:655–9.
[20] Maldonado M, Baybis M, Newman D, et al. Expression of ICAM-1, TNF-alpha, NF-kappa B, and MAP kinase in tubers of the tuberous sclerosis complex. Neurobiol Dis 2003;14:279–90.
[21] Boer K, Crino PB, Gorter JA, et al. Gene expression analysis of tuberous sclerosis complex cortical tubers reveals increased expression of adhesion and inflammatory factors. Brain Pathol 2010;20:704–19.
[22] Crino PB. Evolving neurobiology of tuberous sclerosis complex. Acta Neuropathol 2013;125:317–32.